The Plant Cell, Vol. 20: 2460–2470, September 2008, www.plantcell.org © 2008 American Society of Plant Biologists

Arabidopsis ARC6 Coordinates the Division Machineries of the Inner and Outer Chloroplast Membranes through Interaction with PDV2 in the Intermembrane Space [W]

Jonathan M. Glynn,[a] John E. Froehlich,[b] and Katherine W. Osteryoung[c,1]

[a] Genetics Program, Michigan State University, East Lansing, Michigan 48824
[b] U.S. Department of Energy Plant Research Laboratory, Michigan State University, East Lansing, Michigan 48824
[c] Department of Plant Biology, Michigan State University, East Lansing, Michigan 48824

Chloroplasts arose from a free-living cyanobacterial endosymbiont and divide by binary fission. Division involves the assembly and constriction of the endosymbiont-derived, tubulin-like FtsZ ring on the stromal surface of the inner envelope membrane and the host-derived, dynamin-like ARC5 ring on the cytosolic surface of the outer envelope membrane. Despite the identification of many proteins required for plastid division, the factors coordinating the internal and external division machineries are unknown. Here, we provide evidence that this coordination is mediated in *Arabidopsis thaliana* by an interaction between ARC6, an FtsZ assembly factor spanning the inner envelope membrane, and PDV2, an ARC5 recruitment factor spanning the outer envelope membrane. ARC6 and PDV2 interact via their C-terminal domains in the intermembrane space, consistent with their in vivo topologies. ARC6 acts upstream of PDV2 to localize PDV2 (and hence ARC5) to the division site. We present a model whereby ARC6 relays information on stromal FtsZ ring positioning through PDV2 to the chloroplast surface to specify the site of ARC5 recruitment. Because orthologs of ARC6 occur in land plants, green algae, and cyanobacteria but PDV2 occurs only in land plants, the connection between ARC6 and PDV2 represents the evolution of a plant-specific adaptation to coordinate the assembly and activity of the endosymbiont- and host-derived plastid division components.

INTRODUCTION

The plastids of plant cells arose from cyanobacteria by endosymbiosis and, like cyanobacteria, replicate by binary fission. This process requires the coordinated action of at least two macromolecular complexes, one composed of the tubulin-like cytoskeletal protein FtsZ and the other of the dynamin-related protein ARC5. These proteins assemble into midplastid ring-shaped structures on opposite sides of the two envelope membranes to mediate constriction of the organelle (Miyagishima et al., 2003; Osteryoung and Nunnari, 2003; Maple and Moller, 2007). Two nucleus-encoded plant FtsZ paralogs, FtsZ1 and FtsZ2, function within the chloroplast stroma. Both evolved from cyanobacterial FtsZ and have unique nonoverlapping functions in plastid division (Stokes and Osteryoung, 2003; El-Kafafi et al., 2005, 2008; Maple et al., 2005, 2007; Yoder et al., 2007). Analogous to bacterial FtsZ (Bi and Lutkenhaus, 1991; Goehring and Beckwith, 2005), the plastidic FtsZ proteins assemble at an early step in division to form an equatorial ring, the Z-ring, on the stromal face of the inner envelope membrane (Vitha et al., 2001; Kuroiwa et al., 2002). In bacteria and presumably in plastids, the Z-ring probably functions both as a scaffold for the recruitment of other division proteins and to provide the contractile force needed to pull the membrane inward during constriction (Lan et al., 2007; Li et al., 2007; Osawa et al., 2008).

By contrast, ARC5 was a postsymbiotic adaptation of the eukaryotic host and functions outside the chloroplast (Gao et al., 2003; Miyagishima et al., 2006). ARC5 is a member of the dynamin family of membrane pinchases, best characterized for their roles in endocytic vesicle budding and mitochondrial fission in eukaryotes (McNiven, 1998; Shaw and Nunnari, 2002; Cerveny et al., 2007; Hoppins et al., 2007; Ungewickell and Hinrichsen, 2007), although dynamins probably evolved from a prokaryotic ancestor (Low and Lowe, 2006). ARC5 in *Arabidopsis thaliana* and its ortholog in the red alga *Cyanidioschyzon merolae* function late in chloroplast division by assembling on the cytosolic surface of the outer envelope membrane, where they are thought to perform the final squeeze that aids partitioning of the two daughter organelles (Gao et al., 2003; Miyagishima et al., 2003; Yoshida et al., 2006). Both plastidic FtsZ and ARC5 arose early in the evolution of the chloroplast division machinery, as indicated by their occurrence in both the red and green lineages (Miyagishima, 2005).

The assembly of the division machinery appears to occur in a linear order, with FtsZ assembly initiating the process and ARC5/dynamin mediating late-stage organelle constriction (Miyagishima et al., 2003). However, the mechanisms coordinating these evolutionarily and compartmentally disparate events are unknown. Previous studies in *Arabidopsis* have implicated three plastid

[1] Address correspondence to osteryou@msu.edu.
The author responsible for distribution of materials integral to the findings presented in this article in accordance with the policy described in the Instructions for Authors (www.plantcell.org) is: Katherine W. Osteryoung (osteryou@msu.edu).
[W] Online version contains Web-only data.
www.plantcell.org/cgi/doi/10.1105/tpc.108.061440

division proteins as candidate mediators of this coordination: ARC6, PDV1, and PDV2 (Vitha et al., 2003; Miyagishima et al., 2006). ARC6 is a bitopic transmembrane protein of the inner envelope membrane with its larger N terminus protruding into the stroma and its smaller C terminus residing within the intermembrane space (IMS). ARC6 was inherited from the cyanobacterial endosymbiont and is localized to the midplastid division site. The chloroplasts of *Arabidopsis arc6* mutants, which have one or two oversized chloroplasts per mesophyll cell (Pyke et al., 1994), possess many short disorganized filaments, while *ARC6* overexpressors have excessively long FtsZ filaments (Vitha et al., 2003). These findings, along with the fact that the N terminus of ARC6 interacts specifically with FtsZ2 (Maple et al., 2005), suggest that ARC6 facilitates FtsZ polymer assembly and regulates FtsZ ring dynamics through FtsZ2 (Vitha et al., 2003; Maple et al., 2005; McAndrew et al., 2008). The function of the C-terminal IMS region of ARC6 is unknown, but it probably has a significant role in plastid replication based on the breadth of its conservation among plants, algae, and cyanobacteria (Vitha et al., 2003). Intriguingly, ARC6 is the only protein known to

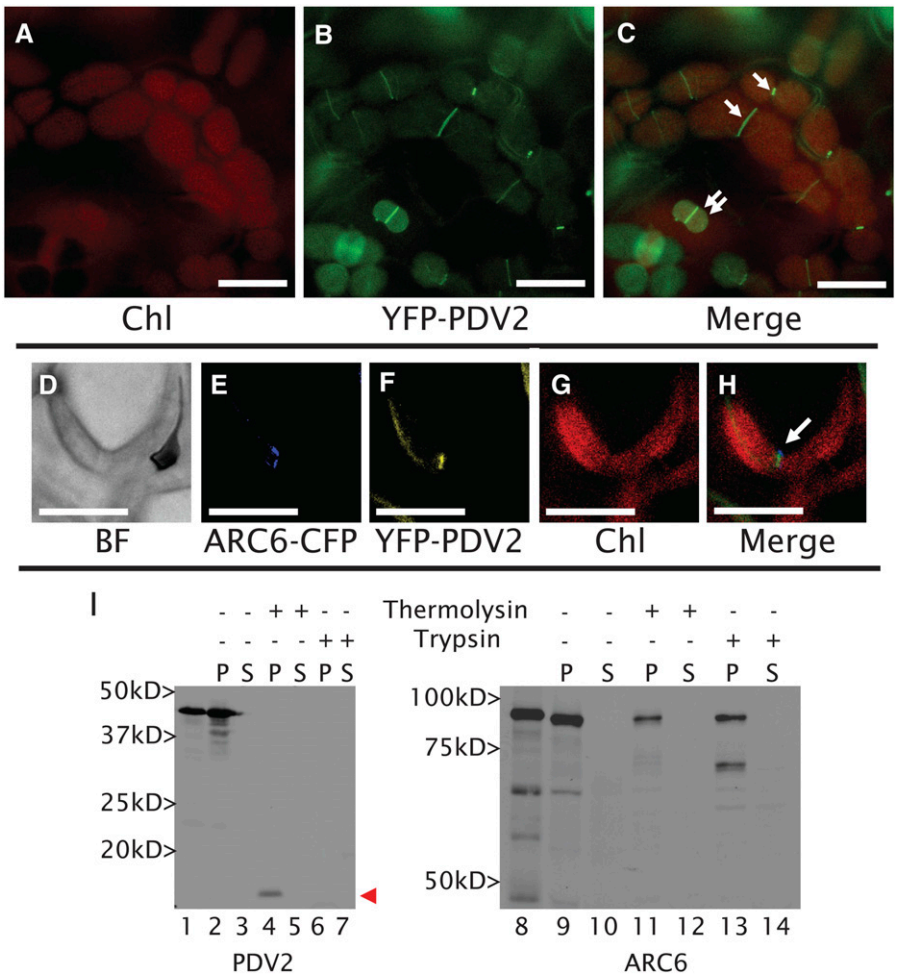

Figure 1. PDV2 Is a Bitopic, Ring-Forming, Plastid-Targeted Protein with an IMS-Localized C Terminus.

(A) to **(C)** Localization of YFP-PDV2 in epidermal cells of *Arabidopsis* young emerging leaves (~4 to 6 mm long) expressing YFP-PDV2 under the control of the *PDV2* promoter sequence. Single arrows point to midplastid PDV2 rings. Double arrows point to smaller plastids with peripheral and ring localization of PDV2.

(D) to **(H)** Colocalization of ARC6-CFP and YFP-PDV2 in the cells of young *Arabidopsis* leaves. Both proteins are expressed under the control of their native promoters.

(I) In vitro chloroplast import of [^{3}H]Leu-labeled PDV2 or [^{35}S]Met-labeled ARC6 and fractionation of chloroplasts following protease treatment and hypotonic lysis. In vitro–transcribed translation products are shown for PDV2 (lane 1) and ARC6 (lane 8). Pellet (P) fractions are shown in lanes 2, 4, 6, 9, 11, and 13. Supernatant (S) fractions are shown in lanes 3, 5, 7, 10, 12, and 14. The arrowhead points to the IMS-localized C-terminal fragment of PDV2 that remains following thermolysin treatment.

BF, bright-field image; ARC6-CFP, fluorescence from ARC6-CFP; YFP-PDV2, fluorescence from YFP-PDV2; Chl, chlorophyll autofluorescence; Merge, merged images from the CFP/YFP/Chl channels. Bars = 10 μm.

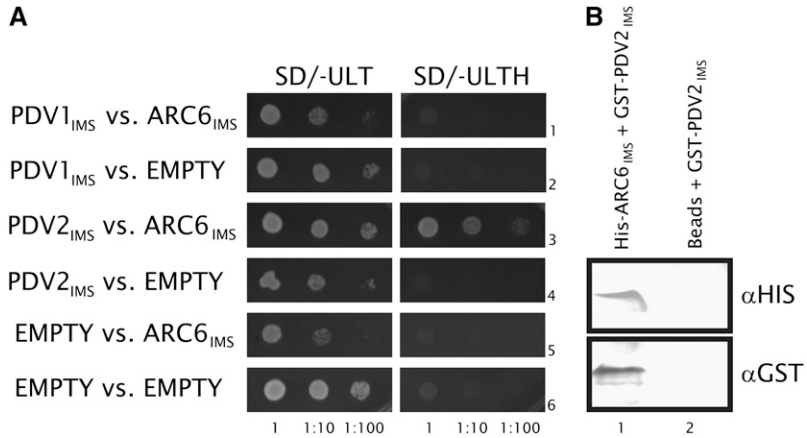

Figure 2. The IMS Regions of ARC6 and PDV2 Interact.

(A) Yeast two-hybrid *HIS3* protein–protein interaction reporter assay showing yeast growth in the presence (SD/−ULT; left panels) or absence (SD/−ULTH; right panels) of His. The $ARC6_{IMS}$, $PDV1_{IMS}$, and $PDV2_{IMS}$ two-hybrid constructs are described in Methods. EMPTY, empty pGBKT7 vector (rows 5 and 6; controls for PDV1 and PDV2) or pGADT7 vector (rows 2, 4, and 6; controls for ARC6). Dilutions from the same starting culture are indicated at bottom.

(B) Immunoblot analysis performed on SDS-PAGE–separated proteins eluted from Ni-Sepharose beads coated with purified His-$ARC6_{IMS}$ and incubated with whole cell extracts expressing GST-$PDV2_{IMS}$ (lane 1) or uncoated beads (Beads) incubated with the same GST-$PDV2_{IMS}$ extracts (lane 2). The blot was probed with anti-His or anti-GST antibodies as indicated.

connect the stromal Z ring to the IMS, suggesting that it could play a critical role in coordinating the inner and outer subassemblies of the division machinery.

PDV1 and PDV2 are paralogous plastid division proteins identified based on the similarity of the *pdv1* mutant phenotype to that of *arc5*; in both mutants, chloroplasts are enlarged and dumbbell-shaped (Miyagishima et al., 2006). PDV1 is a bitopic outer envelope membrane protein that localizes to the division site, with its N terminus residing in the cytosol and its C terminus extending into the IMS. *PDV1* and *PDV2* have partially redundant functions in recruiting ARC5 to the chloroplast. In *pdv1* and *pdv2* mutants, ARC5 localizes to the central constriction in the enlarged chloroplasts, but *pdv1 pdv2* double mutants fail to recruit ARC5 to the chloroplast (Miyagishima et al., 2006). PDV1 and PDV2 proteins share some degree of sequence similarity and domain arrangement, although the localization and detailed function of PDV2 have not been previously determined (Miyagishima et al., 2006). PDV1 and PDV2 have no significant sequence similarity to known proteins and are only evident in land plants, suggesting that they represent an evolutionary development in the transition of plants to terrestrial habitats.

Here, we show that PDV2 has a localization and topology similar to that of PDV1 in the outer envelope membrane. However, PDV2 family members have a unique C-terminal extension in their IMS regions that is lacking in PDV1 proteins. We further show that the C-terminal IMS regions of ARC6 and PDV2 interact and that this interaction is required for full chloroplast division activity in *Arabidopsis*. Using genetic analysis, we demonstrate

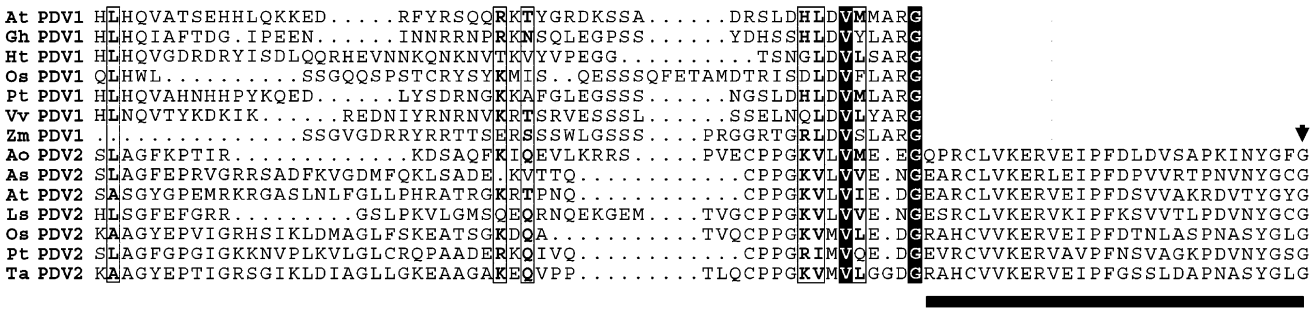

Figure 3. PDV2 Family Members Possess a Unique C-Terminal Extension Not Found in PDV1 Family Members.

A portion of the full-length multiple sequence alignment (see Supplemental Figure 1B online) corresponding to the IMS domains of PDV1 and PDV2 is shown. The PDV2 C-terminal extension is indicated by the horizontal black bar, and the conserved C-terminal Gly of PDV2 is marked with an arrow. The outlined vertical boxed areas represent conserved residues, and the shaded boxed areas represent identical residues shared between PDV1 and PDV2 family members. For full species names of aligned sequences, see the Accession Numbers section at the end of Methods.

that ARC6 is required for positioning of PDV2 and ARC5, but PDV2 is not required for the midplastid localization of ARC6. Our results establish a physical link across the envelope membranes at the division site and suggest that ARC6, through interaction with PDV2 within the IMS, coordinates Z ring and ARC5 activity to synchronize scission of the envelope membranes. We present a model for the physical arrangement and interaction of these proteins in the chloroplast membranes.

RESULTS

PDV2 Localization and Topology Are Similar to Those of PDV1

The similarity of PDV2 to PDV1 in sequence and domain arrangement (see Supplemental Figures 1A to 1C online) suggested that PDV2 localization and topology are similar to those of PDV1 (Miyagishima et al., 2006). To determine the localization of PDV2 in vivo, we expressed a yellow fluorescent protein (YFP)–PDV2 fusion protein from the *PDV2* promoter (*PDV2*$_{pro}$-*YFP-PDV2*) in ecotype Columbia (Col-0) *Arabidopsis* plants. Similar to PDV1, the YFP signal localized to the midplastid in young emerging leaves (Figures 1A to 1C). The YFP-PDV2 signal appeared as a continuous ring rather than as a series of ordered spots, as was previously noted for PDV1 (Miyagishima et al., 2006). When YFP-PDV2 was coexpressed with an ARC6–cyan fluorescent protein (CFP) fusion protein, their fluorescence signals colocalized within mesophyll chloroplasts (Figures 1E to 1H). To confirm the predicted topology of PDV2, we performed in vitro chloroplast import and protease protection assays (Figure 1I, left). Following incubation with isolated pea (*Pisum sativum*) chloroplasts, radiolabeled PDV2 produced by in vitro translation (Figure 1I, lane 1) was retained in the membrane fraction, indicating its association with chloroplasts, but was not processed to a smaller size (Figure 1I, lane 2), consistent with the lack of a predicted transit peptide (Miyagishima et al., 2006). The protein was susceptible to degradation by thermolysin, which cannot penetrate the chloroplast outer envelope, consistent with PDV2 localization in the outer envelope. However, a portion of

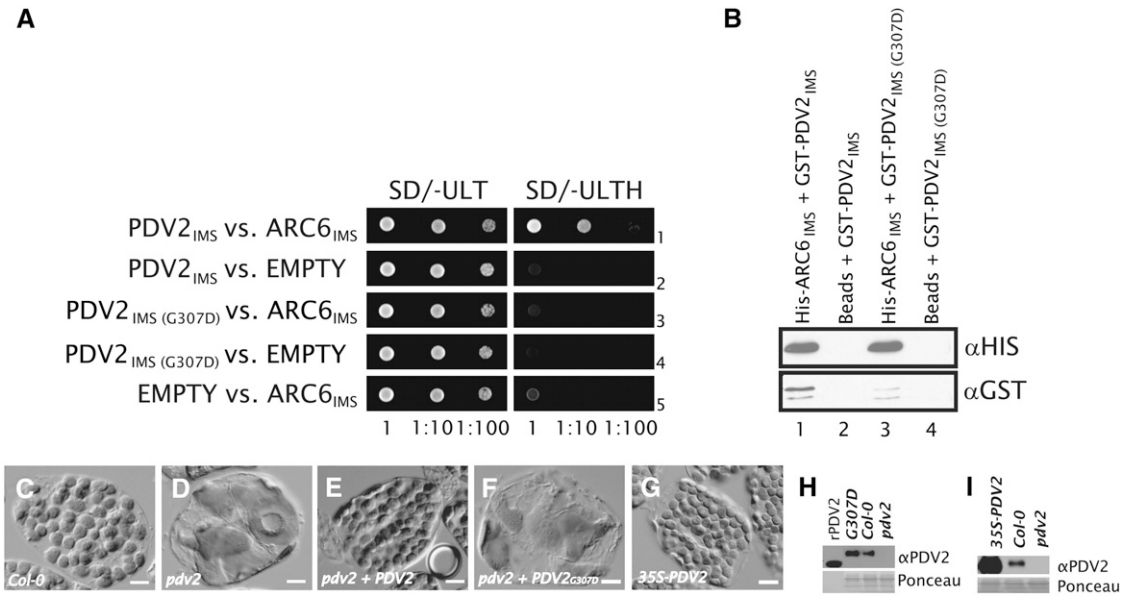

Figure 4. The C-Terminal Gly of PDV2 Is Required for PDV2 Function.

(A) Two-hybrid *HIS3* reporter assay showing yeast growth in the presence (SD/−ULT) or absence (SD/−ULTH) of His. Dilutions from the same starting culture are indicated at bottom. The ARC6$_{IMS}$, PDV2$_{IMS}$, and PDV2$_{IMS(G307D)}$ constructs are described in Methods. EMPTY, empty pGADT7 or pGBKT7 vector.

(B) Immunoblot analysis confirming the ARC6–PDV2 interaction by pull-down assay. Ni-Sepharose beads were coated with purified His-ARC6$_{IMS}$ (lanes 1 and 3) or treated with buffer only (Beads; lanes 2 and 4). Beads were then incubated with crude extracts from *E. coli* cells expressing either GST-PDV2$_{IMS}$ (GST-PDV2; lanes 1 and 2) or GST-PDV2$_{IMS(G307D)}$ (lanes 3 and 4). Protein was eluted and analyzed by immunoblotting as described in Methods.

(C) to **(G)** Phenotype of mesophyll cells in Col-0 **(C)**, *pdv2-1* **(D)**, and *pdv2-1* complemented with a wild-type transgene **(E)**, in *pdv2-1* expressing *PDV2*$_{pro}$-*PDV2*$_{G307D}$ at levels greater than that of Col-0 **(F)**, and in Col-0 expressing *35S*$_{pro}$-*PDV2* **(G)**. Bars = 10 μM.

(H) Immunoblot showing relative PDV2 protein levels in the lines shown in **(C)**, **(D)**, and **(F)**. rPDV2, recombinant antigen (PDV2 amino acids 1 to 212) used for anti-PDV2 production; G307D, whole cell extracts from transgenic plants (representative cell shown in **[F]**) expressing the *PDV2*$_{pro}$-*PDV2*$_{G307D}$ transgene in the *pdv2-1* background; Col-0, whole cell extracts from Col-0; *pdv2*, whole cell extracts from a *pdv2-1* mutant.

(I) Immunoblot showing relative PDV2 protein levels in whole cell extracts from a PDV2 overexpressor line (shown in **[G]**) relative to controls (**[C]** and **[D]**). *35S-PDV2*, whole cell extracts from a transgenic line expressing a *35S*$_{pro}$-*PDV2* transgene; Col-0, whole cell extracts from Col-0; *pdv2*, whole cell extracts from a *pdv2-1* mutant.

PDV2, roughly corresponding to the size of the predicted C-terminal IMS domain (~10 kD; see Supplemental Figure 1A online), was protected from thermolysin degradation (Figure 1I, lane 4, arrowhead) but was sensitive to trypsin, which can penetrate the outer envelope membrane and enter the IMS (Tranel et al., 1995; Jackson et al., 1998). ARC6, used as an inner envelope control in these experiments (Figure 1I, right), behaved as shown previously (Vitha et al., 2003); incubation with chloroplasts produced a slightly smaller protein, indicating import and transit peptide processing, and the import product was membrane-associated and partially protected from trypsin, as expected for a bitopic chloroplast inner envelope membrane protein with an IMS domain. These results confirm that PDV2, like PDV1, is a midplastid-localized, bitopic protein of the chloroplast outer envelope membrane, with its large N terminus exposed to the cytosol and its smaller C terminus residing within the intermembrane space.

The IMS Regions of ARC6 and PDV2 Interact

The similar localization patterns of PDV1 (Miyagishima et al., 2006), PDV2, and ARC6 at the division site, along with their demonstrated topological orientations in the envelope membranes, suggested the possibility that ARC6 might interact with PDV1 and/or PDV2 in the IMS. To test this, we performed yeast two-hybrid assays with constructs encoding the C-terminal IMS domains of ARC6 and PDV1 or PDV2. $PDV2_{IMS}$ strongly and specifically activated the *HIS3* reporter in the presence of $ARC6_{IMS}$ (Figure 2A, third row). No interaction was observed between $PDV1_{IMS}$ and $ARC6_{IMS}$ (Figure 2A, first row), although we cannot rule out the possibility of their direct interaction in vivo. To confirm the $ARC6_{IMS}$–$PDV2_{IMS}$ interaction, we performed a coprecipitation assay (Figure 2B). A glutathione *S*-transferase (GST)–$PDV2_{IMS}$ fusion protein was precipitated from crude *Escherichia coli* extracts with Ni-Sepharose beads coated with His-$ARC6_{IMS}$ (Figure 2B, lane 1), but no pulldown of GST-$PDV2_{IMS}$ was observed using uncoated Ni-Sepharose beads (Figure 2B, lane 2). These results support an ARC6-PDV2 protein–protein interaction within the intermembrane space of dividing chloroplasts.

PDV2 Family Members Contain a Unique C-Terminal IMS Domain

We compared the C-terminal IMS domains of PDV1 and PDV2 in order to gain insight into features that distinguish them from one another and to identify features that might be important for the PDV2-specific interaction with ARC6. We generated a sequence alignment between PDV1 and PDV2 proteins from several land plants using a ClustalW identity-scoring matrix (Larkin et al., 2007) and used this alignment to clearly define PDV1-specific and PDV2-specific features (see Supplemental Figure 1B online). As noted previously, all PDV1 proteins have a conserved C-terminal Gly residue, and mutation of this residue impairs PDV1 function in *Arabidopsis* (Miyagishima et al., 2006). A conserved terminal Gly is also found in all known PDV2 family members (Figure 3, arrow). However, PDV2 proteins have a conserved 28–amino acid extension at their C terminus and thus are generally longer (294 ± 15 amino acids, $n = 7$ sequences) than PDV1 proteins (261 ± 14 amino acids, $n = 7$ sequences). This C-terminal extension, which includes the terminal Gly residue, is likely to mediate the PDV2-specific interaction with ARC6.

The Conserved Gly at the End of the PDV2 C-Terminal Extension Is Required Both for Interaction with $ARC6_{IMS}$ and for PDV2 Function in Vivo

To ask whether the C-terminal Gly of PDV2 is important for the ARC6–PDV2 interaction, we engineered a missense mutation in the $PDV2_{IMS}$ two-hybrid plasmid that changes this Gly to Asp (G307D). Following cotransformation of the resulting construct [$PDV2_{IMS(G307D)}$] and $ARC6_{IMS}$ into yeast and selection for both

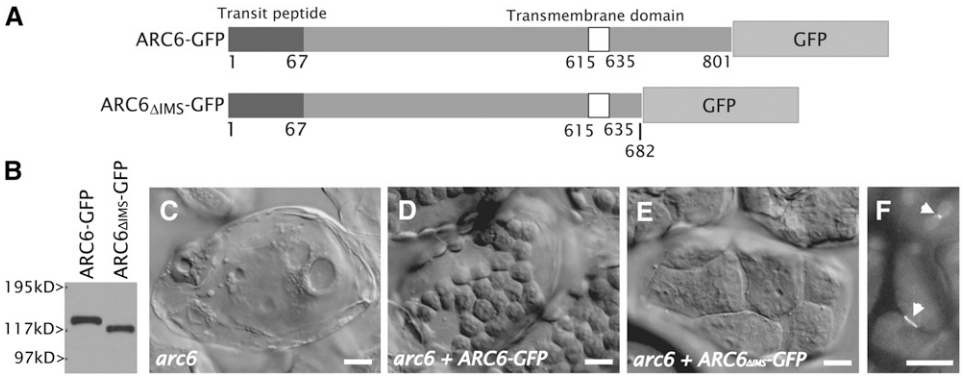

Figure 5. The C-Terminal IMS Region of ARC6 Is Required for Chloroplast Division Activity but Not for ARC6 Localization.

(A) Schemes showing ARC6-GFP and $ARC6_{\Delta IMS}$-GFP. The numbers shown beneath the diagrams indicate amino acid positions.
(B) Anti-GFP immunoblot showing relative GFP fusion protein levels in plants shown in **(D)** and **(E)**.
(C) to **(E)** Phenotypes of an untransformed *arc6* mutant **(C)**, an *arc6* mutant expressing $ARC6_{pro}$-*ARC6-GFP* **(D)**, and *arc6* mesophyll cells expressing $ARC6_{pro}$-$ARC6_{\Delta IMS}$-*GFP* **(E)**. Bars = 10 μM.
(F) GFP localization in *arc6* mutants expressing $35S_{pro}$-$ARC6_{\Delta IMS}$-*GFP*. Arrowheads indicate ring localization of $ARC6_{\Delta IMS}$-GFP at sites of constriction within the chloroplasts of young leaf cells. Bar = 10 μM.

plasmids, we observed no growth on medium lacking His (Figure 4A, row 3), indicating that mutation of the terminal Gly in PDV2 diminishes the $ARC6_{IMS}$–$PDV2_{IMS}$ interaction in yeast (cf. Figure 4A, row 1). We incorporated the same mutation into $PDV2_{IMS}$ to create GST-$PDV2_{IMS(G307D)}$ for use in pull-down assays and observed that the terminal G307D mutation reduced the affinity of $PDV2_{IMS}$ for $ARC6_{IMS}$ (Figure 4B, lane 3). The higher affinity of GST-$PDV2_{IMS}$ for His-$ARC6_{IMS}$ (Figure 4, lane 1) was not the result of biased prey input into the reaction, as equal amounts of total protein were applied to each coprecipitation reaction and we verified equal input levels of GST-$PDV2_{IMS}$ and GST-$PDV2_{IMS(G307D)}$ in the reactions by anti-GST immunoblotting (see Supplemental Figure 2 online). We conclude from these results that the IMS-localized domains of ARC6 and PDV2 interact with each other and that the conserved terminal Gly of PDV2 is important for this interaction.

To assess the potential importance of the terminal missense mutation in vivo, we compared the relative abilities of *$PDV2_{pro}$-PDV2* and *$PDV2_{pro}$-$PDV2_{G307D}$* transgenes encoding full-length proteins to complement *pdv2-1*, an *Arabidopsis* T-DNA insertion allele of *PDV2* in which chloroplasts are frequently constricted and larger than in the wild type (Miyagishima et al., 2006) (cf. Figures 4C and 4D). We reasoned that a PDV2 protein incapable of interaction with ARC6 would not be able to rescue the *pdv2* phenotype. The wild-type transgene fully complemented *pdv2* in the majority of selected lines (Figure 4E). By contrast, no modification of the *pdv2* phenotype occurred in lines transformed with *$PDV2_{pro}$-$PDV2_{G307D}$* (Figure 4F), despite evidence based on immunoblotting with a PDV2-specific antibody that $PDV2_{G307D}$ protein levels were equivalent to or greater than PDV2 levels in the wild type (Figure 4H; see Supplemental Figure 3 online). Lack of complementation was not a consequence of overexpression, because expression of *PDV2* under the control of the *35S* promoter in a wild-type background does not cause defects in chloroplast division or morphology (Figures 4G and 4I). We conclude that PDV2 interaction with ARC6 through the conserved C-terminal Gly is essential for the accumulation of normal chloroplast numbers in *Arabidopsis* leaf cells.

The C-Terminal IMS Region of ARC6 Is Required for Chloroplast Division Activity but Not for ARC6 Localization

To determine if the C-terminal IMS-localized region of ARC6 is required for plastid division in vivo, as suggested by its interaction with PDV2, we expressed a truncated ARC6-GFP

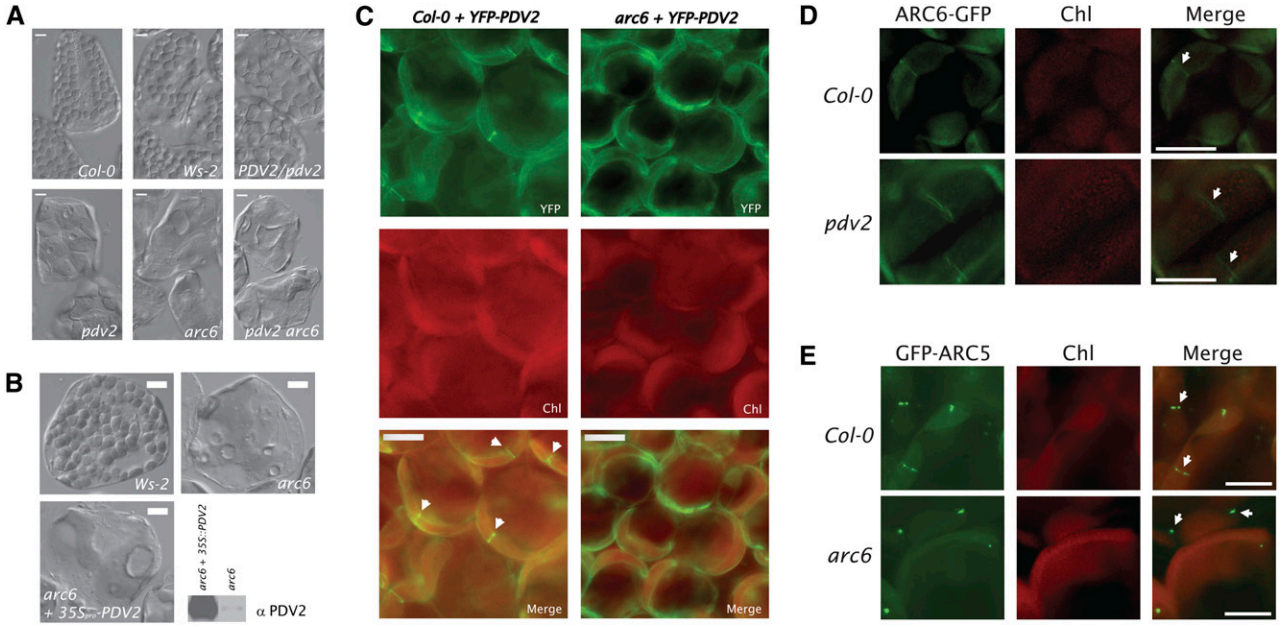

Figure 6. *ARC6* Acts Upstream of *PDV2*.

(A) Phenotypes observed in the F2 population from *arc6-1* × *pdv2-1* reciprocal crosses. *arc6 pdv2* double mutants were confirmed by PCR-based genotyping and were phenotypically indistinguishable from *arc6* mutants.

(B) Phenotypes of mesophyll cells from Wassilewskija-2 (Ws-2; top left), *arc6-1* (top right), and *arc6-1* transformed with *$35S_{pro}$-PDV2* and expressing high levels of PDV2 protein (bottom left). Relative PDV2 protein levels in *arc6-1* and *arc6-1* mutants expressing *$35S_{pro}$*-PDV2 are shown by immunoblot (bottom right).

(C) Localization of YFP-PDV2 in young leaf cells of Col-0 (left panels) and in an *arc6* T-DNA mutant (SAIL_693_G04; right panels). Arrowheads indicate midplastid YFP-PDV2 rings.

(D) Localization of ARC6-GFP in young leaf cells of Col-0 (top panels) and *pdv2-1* (bottom panels). Arrows indicate midplastid ARC6-GFP rings.

(E) Localization of GFP-ARC5 in young leaf cells of Col-0 (top panels; arrows indicate midplastid GFP-ARC5 localization) and in an *arc6-1* mutant (bottom panels; arrows indicate cytosolic GFP-ARC5 patches).

Bars = 10 μM.

fusion protein lacking the conserved portion (Vitha et al., 2003) of its C-terminal IMS region ($ARC6_{\Delta IMS}$-GFP) in the *arc6* background under the control of the *ARC6* promoter (Figure 5A). A full-length *ARC6-GFP* transgene, shown previously to complement the severe chloroplast division defect in *arc6* mutants (Vitha et al., 2003), was expressed as a control. Accumulation of the fusion proteins in transgenic individuals was confirmed by immunoblotting (Figure 5B), and chloroplast morphology was examined in fixed leaf cells. Similar to previous results (Vitha et al., 2003), we observed rescue of the *arc6* phenotype (Figure 5C) in lines expressing full-length ARC6-GFP (Figure 5D), as indicated by the increase in number and the decrease in size of the chloroplasts (25 to 60 chloroplasts/cell; Figure 5D) relative to those in the parent *arc6* plants (1 to 2 chloroplasts/cell; Figure 5C). A change in chloroplast number and size was also observed in lines expressing $ARC6_{\Delta IMS}$-GFP, but the extent to which the *arc6* mutant was complemented (4 to 10 chloroplasts/cell; Figure 5E) was less than that observed in *arc6* lines expressing the full-length *ARC6-GFP* control. These results show that the IMS region of ARC6 is required for full plastid division activity in vivo. Interestingly, *arc6* plants expressing $35S_{pro}$-$ARC6_{\Delta IMS}$-*GFP* (Figure 5F) or $ARC6_{pro}$-$ARC6_{\Delta IMS}$-*GFP* (see Supplemental Figure 4 online) exhibit GFP rings localized to sites of constriction in chloroplasts of young leaves, indicating that the C-terminal IMS region of ARC6 is not required for midplastid localization of ARC6.

ARC6 Acts Upstream of *PDV2*

The findings that $ARC6_{\Delta IMS}$-GFP localizes to the plastid division site and that *arc6* plants expressing $ARC6_{\Delta IMS}$-GFP phenocopy *pdv2* mutants suggested that *ARC6* acts upstream of *PDV2*. Since the phenotypes of *arc6* (one to two chloroplasts per cell) and *pdv2* (four to eight chloroplasts per cell) mutants are easily distinguished by microscopic observation (Figure 6A), we made reciprocal crosses to test for epistasis between the *arc6-1* (Wassilewskija-2 background) and *pdv2-1* (Col-0 background) alleles. F1 individuals were allowed to self-fertilize, and the chloroplast phenotypes in leaves of 105 F2 individuals were examined (Figure 6A). We observed all of the expected phenotypes in the F2 population, including individuals with wild-type phenotypes, intermediate phenotypes consistent with *PDV2*/*pdv2* heterozygotes (Miyagishima et al., 2006), *pdv2*-like phenotypes, and *arc6*-like phenotypes in an ~9:3:4 ratio (phenotypic distribution: wild type + intermediate = 63; *pdv2*-like = 17; *arc6*-like = 25 [$\chi^2 \cong 0.7$; $df = 2$; $P \geq 0.9$]). Genotype analysis of individuals with *arc6*-like phenotypes confirmed the presence of *arc6 pdv2* double mutants within the F2 population (Figure 6A). The overrepresentation of *arc6* mutant phenotypes in the F2 population and the *arc6*-like phenotype of the *arc6 pdv2* double mutant are consistent with *ARC6* acting upstream of *PDV2*.

To further investigate the dependence of PDV2 function on ARC6, we introduced a T-DNA carrying $35S_{pro}$-*PDV2* into the *arc6* mutant to ask whether overexpression of PDV2 would abrogate the *arc6* phenotype. Following selection, we assayed T1 individuals for PDV2 protein levels by immunoblotting and identified multiple lines with elevated PDV2 levels (Figure 6B, bottom right). In none of these PDV2-overexpressing lines did we observe significant modification of the *arc6* phenotype (Figure 6B, top right); mesophyll cells from all PDV2 overexpressors still contained only one or two oversized chloroplasts (Figure 6B, bottom left). This result indicates that ARC6 is required for PDV2 function and that overexpression of PDV2 is unable to compensate for the loss of ARC6.

ARC6 Is Required for Equatorial Positioning of PDV2 and ARC5

The findings that ARC6 acts upstream of PDV2 and interacts with PDV2 suggested that ARC6 might play a role in PDV2 positioning at the division site. To test this hypothesis, we introduced a transgene carrying $PDV2_{pro}$-*YFP-PDV2* into Col-0 and into an *arc6* T-DNA insertion mutant (SAIL_693_G04) and examined YFP localization in young leaves of T1 individuals. In the wild-type background, we observed equatorial rings of YFP-PDV2 in 34% of chloroplasts (Figure 6C, left; $n = 200$ chloroplasts from 20 independent T1 individuals). By contrast, in the *arc6* background, all lines expressing YFP-PDV2 exhibited diffuse YFP localization around the periphery of the chloroplasts, and no YFP-PDV2 rings were observed (Figure 6C, right; $n = 200$ chloroplasts from 16 T1 individuals). In the converse experiment, we examined ARC6-GFP localization in wild-type and *pdv2* backgrounds (Figure 6D). In both cases, ARC6-GFP was observed in equatorial rings, indicating that PDV2 does not influence ARC6 localization. We conclude that PDV2 is targeted to the outer envelope in an ARC6-independent manner but requires ARC6 for its localization to the division site.

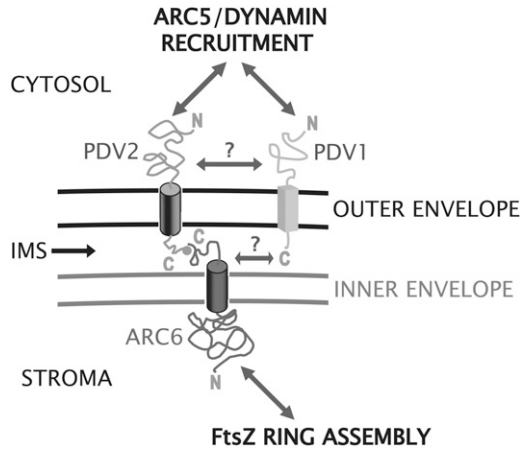

Figure 7. Model for the Coordination of the Inner and Outer Envelope Division Machineries.

ARC6 positioning is probably determined by Z ring position. ARC6 functions in part to regulate FtsZ filament formation. The C-terminal IMS region of ARC6 interacts directly with the C-terminal IMS region of PDV2 and positions PDV2 at the division site. PDV2, a dynamin recruitment protein, directs ARC5 localization and ring formation at the site of constriction in concert with PDV1. ARC6 may also position PDV1 at the division site, perhaps indirectly through an unknown factor (?). The connection between PDV2 and PDV1 is unclear (?) at this time.

To extend this analysis and further elucidate the role of ARC6 in mediating dynamin recruitment through PDV1-PDV2, we examined GFP-ARC5 localization in wild-type cells and *arc6* mutants (Figure 6E). In young wild-type leaf cells, GFP-ARC5 was frequently observed in a punctate pattern around the division site (Figure 6E, top row). By contrast, we observed GFP-ARC5 in patches within the *arc6-1* mutant that do not appear to be associated with chloroplasts (Figure 6E, bottom row), similar to the reported GFP-ARC5 localization in the *pdv1 pdv2* double mutant (Miyagishima et al., 2006). These patches are probably cytosolic (Miyagishima et al., 2003). Since GFP-ARC5 still localizes to the division site in a *pdv2* mutant (Miyagishima et al., 2006), we conclude that ARC6 mediates dynamin recruitment and patterning through both PDV1 and PDV2 but that ARC6 might influence PDV1 function through an indirect mechanism.

DISCUSSION

Chloroplast division involves the consecutive formation and coordinated constriction of the midplastid FtsZ and ARC5/dynamin rings on the stromal and cytosolic surfaces of the envelope membranes, respectively. ARC6 in the inner envelope interacts directly with FtsZ via its stroma-exposed N terminus and is required for Z ring assembly, while PDV2, shown here to be a transmembrane protein of the outer envelope, mediates the recruitment of ARC5 to the chloroplast surface (Vitha et al., 2003; Maple et al., 2005; Miyagishima et al., 2006). Our results place *ARC6* upstream of *PDV2* in the chloroplast division process, identify a physical linkage between the C-terminal IMS domains of ARC6 and PDV2, and reveal that an important function of the ARC6 IMS domain is to direct the localization of PDV2 to the division site. These findings establish a role for a key inner envelope plastid division protein in organizing components of the outer envelope division machinery. Because the N terminus of ARC6 plays a role in organizing FtsZ in the stroma (Vitha et al., 2003), these findings suggest a model wherein interaction between ARC6 and PDV2 within the IMS links FtsZ assembly with ARC5 recruitment, thereby promoting coordinated fission of the two envelope membranes.

Our observation that ARC6 is able to localize to the division site without its IMS region (Figure 5F) suggests that stromal factors are sufficient to organize ARC6 at the division site within chloroplasts. The FtsZ ring is a strong candidate as an ARC6 positioning factor. The recently demonstrated ability of recombinant *E. coli* FtsZ to assemble into rings inside liposomes suggests that FtsZ proteins, which are highly conserved across kingdoms (Vaughan et al., 2004), require only a membrane tether and GTP for ring assembly in vivo (Osawa et al., 2008). We suspect that self-assembly of the Z ring at the midplastid division site in plants, controlled by MinD, MinE, and ARC3 (Glynn et al., 2007; Maple and Moller, 2007), establishes the site for ARC6 localization, presumably via direct interaction with FtsZ2 (Maple et al., 2005). From our results, we propose that ARC6 transduces positional information from the Z ring to the intermembrane space and serves as a landmark for PDV2 and hence ARC5 recruitment (Figure 7). Consistent with this idea, *arc6* plants expressing *ARC6*$_{\Delta IMS}$*-GFP* (Figure 5E) phenocopy *pdv2* and *arc5* mutants (Miyagishima et al., 2006), suggesting an equivalent block in the division process in these three genetically distinct backgrounds. Additionally, the loss of PDV2 or ARC5 results in the formation of multiple adjacent Z rings on the stromal side of the inner envelope membrane (Miyagishima et al., 2006), suggesting that information may also travel inward from the outer envelope to the Z ring through ARC6. Based on the collective data, we hypothesize that ARC6 has evolved to organize and coordinate the stromal and cytosolic components of the division complex and relay information about the status of each across compartment boundaries.

Although PDV1 and PDV2 have partially redundant functions in ARC5 recruitment (Miyagishima et al., 2006), their exact functional relationship in the plastid division complex is not yet clear. In contrast with ARC6 and PDV2, we did not detect an interaction between ARC6 and PDV1 in yeast two-hybrid assays (Figure 2, row 1). However, preliminary experiments suggest that *ARC6* is required for the localization of PDV1 as well as PDV2 (see Supplemental Figure 5 online), consistent with the lack of ARC5 recruitment in an *arc6* mutant (Figure 6E). We do not believe that ARC6-dependent localization of PDV1 is mediated directly by PDV2, because GFP-ARC5 localizes properly in *pdv2-1* (Miyagishima et al., 2006). Rather, the data suggest that another factor acts downstream of ARC6 to position PDV1, and hence ARC5, independently of PDV2 (Figure 7). In this context, it is interesting that PDV1 and PDV2 appear to have distinct localization patterns at the division site: GFP-PDV1 is observed in discrete foci (Miyagishima et al., 2006), whereas YFP-PDV2 is observed as a continuous ring (Figure 1C). The significance of this difference is unknown, but it could reflect their interactions with different positioning factors: ARC6 in the case of PDV2 and an unknown factor in the case of PDV1.

The PDV2-interacting IMS region of ARC6 is mostly conserved with the corresponding region of the ARC6 cyanobacterial ortholog Ftn2, yet PDV2 is not found in cyanobacteria or green algae. Perusal of sequence alignments suggests the presence of land plant–specific motifs within the IMS region of ARC6 that may have evolved in parallel with the emergence of PDV1 and PDV2. Ftn2 is localized to the division site in cyanobacteria (Mazouni et al., 2004) and presumably has a topology similar to that of ARC6 (i.e., its C terminus protrudes into the periplasm). This leads us to ask: did PDV2 replace a periplasmic component of the cyanobacterial divisome (e.g., a component of the peptidoglycan synthesis machinery or the murein layer itself) or does the ARC6–PDV2 interaction represent a new plant-specific function for ARC6? Understanding the functional similarities and differences between ARC6 and Ftn2 will provide further insight into the evolution of the plastid division machinery in plants.

METHODS

Plant Transformation Vectors and Analysis

Arabidopsis thaliana ARC6-GFP and ARC6$_{\Delta IMS}$-GFP coding sequences, corresponding to amino acids 1 to 801 and 1 to 682 of ARC6, respectively, were cloned into pCAMBIA1302 (Hajdukiewicz et al., 1994) or a derivative of pCAMBIA1302 containing the ARC6 promoter region (Vitha et al., 2003) using *Nco*I-*Bgl*II sites for insertion. *PDV2*$_{pro}$*-YFP-PDV2* was generated by

removing the 35S promoter and mGFP-His sequences from pCAMBIA1302 and replacing them with a fragment carrying the PDV2 promoter region and EYFP (Clontech) fused to the PDV2 coding sequence. For ARC6-CFP, *ARC6* was cloned into a derivative of pCAMBIA1302 containing the *ARC6* promoter region (Vitha et al., 2003) and ECFP coding sequence (Clontech). Lines expressing proteins from both *PDV2*$_{pro}$*-YFP-PDV2* and *ARC6*$_{pro}$*-ARC6-CFP* were generated by crossing independently transformed T1 lines (with demonstrated transgene expression) and selecting progeny with YFP and CFP expression. *PDV2*$_{pro}$*-PDV2* and *PDV2*$_{pro}$*-PDV2*$_{G307D}$ were generated by PCR and cloned into a derivative of pCAMBIA1302 that lacks the 35S promoter and GFP coding sequence. All plant transformations were performed as described previously (Miyagishima et al., 2006) using *Agrobacterium tumefaciens* GV3101. Selection of T1 individuals was performed on Linsmaier and Skoog medium (Caisson Laboratories) containing hygromycin (20 to 25 μg/mL).

Microscopy and Image Analysis

Light micrographs depicting chloroplast morphology in expanded leaf cells were taken using differential interference contrast optics on a Leica DMI3000B inverted microscope outfitted with a Leica DFC320 camera. Samples for chloroplast morphology and quantitation were prepared and analyzed using established protocols (Pyke and Leech, 1991). Fluorescence micrographs were taken using a Leica DMRA2 microscope using Q-Capture camera control software (Q-Imaging) and the filter sets indicated (Leica) as described previously (Vitha et al., 2003). Image analysis and RGB composites were made using ImageJ version 1.37 (National Institutes of Health).

Two-Hybrid Analysis

Yeast strain AH109 (Clontech) was cultured and transformed as recommended by the manufacturer using standard Synthetic Dropout medium (Clontech) as indicated. The coding sequence for ARC6 amino acids 637 to 801 was cloned into pGADT7 using *Nde*I-*Xma*I sites to create ARC6$_{IMS}$. The coding sequence for PDV1 amino acids 226 to 272 was cloned into pGBKT7 using *Nde*I-*Xma*I sites to create PDV1$_{IMS}$. The coding sequence for PDV2 amino acids 233 to 307 was cloned into pGBKT7 using *Nde*I-*Xma*I sites to create PDV2$_{IMS}$. PDV2$_{IMS(G307D)}$ was generated by PCR-based mutagenesis and cloned into pGBKT7 using *Nde*I-*Xma*I sites.

Pull-Down Assays

Recombinant His-ARC6$_{IMS}$ (encoding ARC6 amino acids 637 to 801 with an N-terminal 8× His tag) was generated in pHIS8-3 (Salk Institute) and expressed in BL21 (DE3) Codon Plus cells (Stratagene). Isopropylthio-β-galactoside (2 mM) was applied to the cells at $OD_{600} \sim 0.8$ and incubated for 4 h to generate the His8-ARC6$_{IMS}$ fusion protein. Total protein was extracted from the induced cells by sonication in buffer A (1× Tris-buffered saline [TBS], 40 mM imidazole, and one tablet of EDTA-free protease inhibitor cocktail [Roche; 11836170001] per 100 mL of buffer A) followed by treatment of the sonicated material with 0.5% Triton X-100 for 30 min at room temperature. After centrifugation at 18,000*g*, the supernatant was collected and analyzed by Bradford assay (Bio-Rad). Total protein (750 μg) was applied to 50 μL of Ni-Sepharose beads equilibrated in buffer A (Ni-Sepharose 6 Fast Flow; GE Healthcare). Beads were washed four times in buffer A to enrich for His-ARC6$_{IMS}$. Negative controls (beads only) were simply washed in buffer A following equilibration. Production of crude GST-PDV2$_{IMS}$ (encoding PDV2 amino acids 233 to 307 with an N-terminal GST tag) and GST-PDV2$_{IMS(G307D)}$ (identical to PDV2$_{IMS}$, except that a Gly-to-Asp change was introduced in the coding sequence for the C-terminal residue of PDV2) was performed using the methods described above, except that pGEX-4T-2 (GE Healthcare) was used as the parent vector for cloning and expression of recombinant PDV2 proteins. The cell extracts containing the GST fusions were prepared by sonication and treatment with Triton X-100 and then centrifuged to yield a crudely purified sample. Total protein was measured by Bradford assay, and 750 μg of total protein was applied to the naked Ni-Sepharose beads or Ni-Sepharose beads coated with His-ARC6$_{IMS}$. Following a 2.5-h incubation on a rocking platform, the samples were washed several times with buffer A and then eluted into 250 μL of buffer B (buffer A containing 1 M imidazole). Approximately 240 μL of eluate was recovered following a brief spin, and total eluted material was precipitated in acetone and reconstituted in 6× sample buffer prior to separation using SDS-PAGE. Approximately 12.5% of the eluted material was applied in each lane for separation on 15% SDS-polyacrylamide gels. Separated proteins were transferred to nitrocellulose (GE Water and Process Technologies) and blotted with anti-His (Pierce; 15165) or anti-GST (Sigma-Aldrich; G-1417) antibodies as recommended by the manufacturer and then were detected by standard chemiluminescence methods using the manufacturer's horseradish peroxidase–based detection protocol (Pierce).

Immunoblotting of Plant Material

Proteins from whole cell extracts (equivalent to ~2 to 3 mg ground in liquid nitrogen) were prepared as described previously (Weigel and Glazebrook, 2002), separated by SDS-PAGE, and transferred to nitrocellulose. Anti-GFP immunoblotting was performed using Clontech JL-8 anti-GFP monoclonal antibody at 1:1000 in 5% nonfat dry milk in TBS-T, pH 7.4 (Miyagishima et al., 2006). Anti-PDV2 immunoblotting was performed using 1 mg/mL protein A–purified IgGs from New Zealand White rabbit sera (CRP) directed against PDV2 (1:15,000) in 5% nonfat dry milk in TBS-T, pH7.4. Recombinant PDV2 used as the immunogen for anti-PDV2 antibody production was generated by cloning the coding sequence for PDV2 amino acids 1 to 212 into pHIS8-3 (Salk Institute), expressing in BL21 (DE3) Codon Plus cells (Stratagene), and purifying the resulting fusion protein from cell extracts using Ni-Sepharose 6 Fast Flow (GE Healthcare) according to the manufacturer's recommendations.

Phylogenetic Analysis

ClustalW2 was used to generate a multiple sequence alignment using PDV1 and PDV2 sequences from the organisms shown. Scoring was based on an identity matrix with default settings: Protein Gap Open Penalty = 10.0; Protein Gap Extension Penalty = 0.2; Protein ENDGAP = −1; Protein GAPDIST = 4. MEGA version 4.0.2 (Tamura et al., 2007) was used to generate the phylogenetic tree shown in Supplemental Figure 1C online. Branches corresponding to partitions reproduced in fewer than 50% of bootstrap replicates are collapsed. The percentage of replicate trees in which the associated taxa clustered together in the bootstrap test (1000 replicates) is shown next to the branches. The tree is drawn to scale, with branch lengths in the same units as those of the evolutionary distances used to infer the phylogenetic tree. The evolutionary distances were computed using the Poisson correction method and are in units of the number of amino acid substitutions per site. All positions containing gaps and missing data were eliminated from the data set (complete deletion option). There were 148 positions in the final data set.

Chloroplast Import, Fractionation, and Protease Protection Assays

The cDNA for *PDV2* was subcloned into pDEST14 (Invitrogen) according to the manufacturer's protocol prior to in vitro transcription translation. In vitro–produced protein was generated using the Promega TnT coupled reticulocyte lysate system according to the manufacturer's protocol using ^{3}H-labeled Leu (Perkin-Elmer) as a marker for PDV2 and

^{35}S-labeled Met (Perkin-Elmer) as a marker for ARC6 protein. Pea (*Pisum sativum*) chloroplasts were isolated as described previously (Bruce, 1998). Import assays and fractionation were performed according to previously established protocols (Tranel et al., 1995; Jackson et al., 1998; Vitha et al., 2003).

Accession Numbers

Arabidopsis Genome Initiative locus identifiers related to sequences described in this work are as follows: *ARC6* (At5g42480), *PDV1* (At5g53280), *PDV2* (At2g16070), and *ARC5* (At3g19720). Germplasm identification numbers for *arc6* and *pdv2* alleles used in this work are as follows: *arc6-1* (The Arabidopsis Information Resource stock number CS286), SAIL_693_G04 (The Arabidopsis Information Resource stock number CS879651), and *pdv2-1* (SALK_059656). GenBank accession numbers used for multiple sequence alignments and phylogenetic analysis are as follows: *Arabidopsis thaliana* PDV1 (AAM64850), *Gossypium hirsutum* PDV1 (DW511385 and DW512027), *Helianthus tuberosus* PDV1 (EL464676), *Oryza sativa* PDV1 (NP_001042451), *Populus trichocarpa* PDV1 (ABK94742), *Vitis vinifera* PDV1 (CAO69353), *Zea mays PDV1* (EE161990 and DR959634), *Arabidopsis thaliana* PDV2 (NP_028242), *Asparagus officinalis* PDV2 (CV287540), *Aquilegia* sp PDV2 (DT728284 and DT749563), *Lactuca sativa* PDV2 (DY983634), *Oryza sativa* PDV2 (EAZ02618), *Populus trichocarpa* PDV2 (a GENSCAN-based prediction [http://genes.mit.edu/GENSCAN.html] of *Populus trichocarpa* Scaffold LG_IX 3439000 to 3442500), and *Triticum aestivum* PDV2 (CK209373 and BJ311269).

Supplemental Data

The following materials are available in the online version of this article.

Supplemental Figure 1. Multiple Sequence Comparison of PDV1 and PDV2 Family Members.

Supplemental Figure 2. Relative Inputs of GST-PDV2$_{IMS}$ and GST-PDV2$_{IMS(G307D)}$ in Coprecipitation Reactions.

Supplemental Figure 3. Antibody Specificity of anti-PDV2.

Supplemental Figure 4. GFP Localization Pattern in an *arc6* Mutant Expressing *ARC6$_{pro}$-ARC6$_{\Delta IMS}$-GFP*.

Supplemental Figure 5. GFP-PDV1 Localization in an *arc6* Mutant.

ACKNOWLEDGMENTS

We thank Shin-ya Miyagishima, Aaron Schmitz, and Bradley Olson for helpful comments on this work. This project was supported by National Science Foundation Grant 0313520 and U.S. Department of Energy Grant DE-FG-02-06ER15808 to K.W.O. J.E.F. was supported by grants from the National Science Foundation and the U.S. Department of Energy.

Received June 12, 2008; revised August 21, 2008; accepted September 9, 2008; published September 23, 2008.

REFERENCES

Bi, E.F., and Lutkenhaus, J. (1991). FtsZ ring structure associated with division in *Escherichia coli*. Nature **354:** 161–164.

Bruce, B.D. (1998). The role of lipids in plastid protein transport. Plant Mol. Biol. **38:** 223–246.

Cerveny, K.L., Tamura, Y., Zhang, Z., Jensen, R.E., and Sesaki, H. (2007). Regulation of mitochondrial fusion and division. Trends Cell Biol. **17:** 563–569.

El-Kafafi, S., Karamoko, M., Pignot-Paintrand, I., Grunwald, D., Mandaron, P., Lerbs-Mache, S., and Falconet, D. (2008). Developmentally regulated association of plastid division protein FtsZ1 with thylakoid membranes in *Arabidopsis thaliana*. Biochem. J. **409:** 87–94.

El-Kafafi, S., Mukherjee, S., El-Shami, M., Putaux, J.L., Block, M.A., Pignot-Paintrand, I., Lerbs-Mache, S., and Falconet, D. (2005). The plastid division proteins, FtsZ1 and FtsZ2, differ in their biochemical properties and sub-plastidial localization. Biochem. J. **387:** 669–676.

Gao, H., Kadirjan-Kalbach, D., Froehlich, J.E., and Osteryoung, K.W. (2003). ARC5, a cytosolic dynamin-like protein from plants, is part of the chloroplast division machinery. Proc. Natl. Acad. Sci. USA **100:** 4328–4333.

Glynn, J.M., Miyagishima, S.Y., Yoder, D.W., Osteryoung, K.W., and Vitha, S. (2007). Chloroplast division. Traffic **8:** 451–461.

Goehring, N.W., and Beckwith, J. (2005). Diverse paths to midcell: Assembly of the bacterial cell division machinery. Curr. Biol. **15:** R514–R526.

Hajdukiewicz, P., Svab, Z., and Maliga, P. (1994). The small, versatile pPZP family of Agrobacterium binary vectors for plant transformation. Plant Mol. Biol. **25:** 989–994.

Hoppins, S., Lackner, L., and Nunnari, J. (2007). The machines that divide and fuse mitochondria. Annu. Rev. Biochem. **76:** 751–780.

Jackson, D.T., Froehlich, J.E., and Keegstra, K. (1998). The hydrophilic domain of Tic110, an inner envelope membrane component of the chloroplastic protein translocation apparatus, faces the stromal compartment. J. Biol. Chem. **273:** 16583–16588.

Kuroiwa, H., Mori, T., Takahara, M., Miyagishima, S.Y., and Kuroiwa, T. (2002). Chloroplast division machinery as revealed by immunofluorescence and electron microscopy. Planta **215:** 185–190.

Lan, G., Wolgemuth, C.W., and Sun, S.X. (2007). Z-ring force and cell shape during division in rod-like bacteria. Proc. Natl. Acad. Sci. USA **104:** 16110–16115.

Larkin, M.A., et al. (2007). Clustal W and Clustal X version 2.0. Bioinformatics **23:** 2947–2948.

Li, Z., Trimble, M.J., Brun, Y.V., and Jensen, G.J. (2007). The structure of FtsZ filaments in vivo suggests a force-generating role in cell division. EMBO J. **26:** 4694–4708.

Low, H.H., and Lowe, J. (2006). A bacterial dynamin-like protein. Nature **444:** 766–769.

Maple, J., Aldridge, C., and Moller, S.G. (2005). Plastid division is mediated by combinatorial assembly of plastid division proteins. Plant J. **43:** 811–823.

Maple, J., and Moller, S.G. (2007). Plastid division: Evolution, mechanism and complexity. Ann. Bot. (Lond.) **99:** 565–579.

Maple, J., Vojta, L., Soll, J., and Moller, S.G. (2007). ARC3 is a stromal Z-ring accessory protein essential for plastid division. EMBO Rep. **8:** 293–299.

Mazouni, K., Domain, F., Cassier-Chauvat, C., and Chauvat, F. (2004). Molecular analysis of the key cytokinetic components of cyanobacteria: FtsZ, ZipN and MinCDE. Mol. Microbiol. **52:** 1145–1158.

McAndrew, R.S., Olson, B.J., Kadirjan-Kalbach, D.K., Chi-Ham, C. L., Vitha, S., Froehlich, J.E., and Osteryoung, K.W. (2008). In vivo quantitative relationship between plastid division proteins FtsZ1 and FtsZ2 and identification of ARC6 and ARC3 in a native FtsZ complex. Biochem. J. **412:** 367–378.

McNiven, M.A. (1998). Dynamin: A molecular motor with pinchase action. Cell **94:** 151–154.

Miyagishima, S.-y. (2005). Origin and evolution of the chloroplast division machinery. J. Plant Res. **118:** 295-306.

Miyagishima, S.-y., Froehlich, J.E., and Osteryoung, K.W. (2006).

PDV1 and PDV2 mediate recruitment of the dynamin-related protein ARC5 to the plastid division site. Plant Cell **18:** 2517–2530.

Miyagishima, S.-y., Nishida, K., Mori, T., Matsuzaki, M., Higashiyama, T., Kuroiwa, H., and Kuroiwa, T. (2003). A plant-specific dynamin-related protein forms a ring at the chloroplast division site. Plant Cell **15:** 655–665.

Osawa, M., Anderson, D.E., and Erickson, H.P. (2008). Reconstitution of contractile FtsZ rings in liposomes. Science **320:** 792–794.

Osteryoung, K.W., and Nunnari, J. (2003). The division of endosymbiotic organelles. Science **302:** 1698–1704.

Pyke, K.A., and Leech, R.M. (1991). Rapid image analysis screening procedure for identifying chloroplast number mutants in mesophyll cells of *Arabidopsis thaliana* (L.) Heynh. Plant Physiol. **96:** 1193–1195.

Pyke, K.A., Rutherford, S.M., Robertson, E.J., and Leech, R.M. (1994). arc6, a fertile Arabidopsis mutant with only two mesophyll cell chloroplasts. Plant Physiol. **106:** 1169–1177.

Shaw, J.M., and Nunnari, J. (2002). Mitochondrial dynamics and division in budding yeast. Trends Cell Biol. **12:** 178–184.

Stokes, K.D., and Osteryoung, K.W. (2003). Early divergence of the FtsZ1 and FtsZ2 plastid division gene families in photosynthetic eukaryotes. Gene **320:** 97–108.

Tamura, K., Dudley, J., Nei, M., and Kumar, S. (2007). MEGA4: Molecular Evolutionary Genetics Analysis (MEGA) software version 4.0. Mol. Biol. Evol. **24:** 1596–1599.

Tranel, P.J., Froehlich, J., Goyal, A., and Keegstra, K. (1995). A component of the chloroplastic protein import apparatus is targeted to the outer envelope membrane via a novel pathway. EMBO J. **14:** 2436–2446.

Ungewickell, E.J., and Hinrichsen, L. (2007). Endocytosis: Clathrin-mediated membrane budding. Curr. Opin. Cell Biol. **19:** 417–425.

Vaughan, S., Wickstead, B., Gull, K., and Addinall, S.G. (2004). Molecular evolution of FtsZ protein sequences encoded within the genomes of archaea, bacteria, and eukaryota. J. Mol. Evol. **58:** 19–29.

Vitha, S., Froehlich, J.E., Koksharova, O., Pyke, K.A., van Erp, H., and Osteryoung, K.W. (2003). ARC6 is a J-domain plastid division protein and an evolutionary descendant of the cyanobacterial cell division protein Ftn2. Plant Cell **15:** 1918–1933.

Vitha, S., McAndrew, R.S., and Osteryoung, K.W. (2001). FtsZ ring formation at the chloroplast division site in plants. J. Cell Biol. **153:** 111–120.

Weigel, D., and Glazebrook, J. (2002). *Arabidopsis*: A Laboratory Manual. (Cold Spring Harbor, NY: Cold Spring Harbor Laboratory Press).

Yoder, D.W., Kadirjan-Kalbach, D., Olson, B.J., Miyagishima, S.Y., Deblasio, S.L., Hangarter, R.P., and Osteryoung, K.W. (2007). Effects of mutations in Arabidopsis FtsZ1 on plastid division, FtsZ ring formation and positioning, and FtsZ filament morphology in vivo. Plant Cell Physiol. **48:** 775–791.

Yoshida, Y., Kuroiwa, H., Misumi, O., Nishida, K., Yagisawa, F., Fujiwara, T., Nanamiya, H., Kawamura, F., and Kuroiwa, T. (2006). Isolated chloroplast division machinery can actively constrict after stretching. Science **313:** 1435–1438.

Arabidopsis ARC6 Coordinates the Division Machineries of the Inner and Outer Chloroplast Membranes through Interaction with PDV2 in the Intermembrane Space
Jonathan M. Glynn, John E. Froehlich and Katherine W. Osteryoung
Plant Cell 2008;20;2460-2470; originally published online September 23, 2008;
DOI 10.1105/tpc.108.061440

This information is current as of July 19, 2018

Supplemental Data	**/content/suppl/2008/09/15/tpc.108.061440.DC1.html**
References	This article cites 39 articles, 14 of which can be accessed free at: /content/20/9/2460.full.html#ref-list-1
Permissions	https://www.copyright.com/ccc/openurl.do?sid=pd_hw1532298X&issn=1532298X&WT.mc_id=pd_hw1532298X
eTOCs	Sign up for eTOCs at: http://www.plantcell.org/cgi/alerts/ctmain
CiteTrack Alerts	Sign up for CiteTrack Alerts at: http://www.plantcell.org/cgi/alerts/ctmain
Subscription Information	Subscription Information for *The Plant Cell* and *Plant Physiology* is available at: http://www.aspb.org/publications/subscriptions.cfm

© American Society of Plant Biologists
ADVANCING THE SCIENCE OF PLANT BIOLOGY